

# The Newcastle Dilatometer Testing in Pakistani Sandy Subsoils

A. Akbar

Professor, Civil Engineering Department, University of Engineering and Technology, Lahore Pakistan

H. Nawaz

Research Student, Civil Engineering Department, University of Engineering and Technology, Lahore

B.G. Clarke

Professor of Geotechnical Engineering, Newcastle University, UK

Keywords: dilatometer, sand, shear strength, stiffness

**ABSTRACT:** The Newcastle Flat Rigid Dilatometer (*NDMT*) is a new in-situ soil testing device developed in 2001 for direct measurement of the in-situ characteristics of soils such as strength, stiffness, deformation etc. It is quite simple and robust and produces repeatable calibration data with no hysteresis. The *NDMT* loads the soil with a relatively rigid piston of 3 mm thickness so that it can be used in all soils including those containing gravel. The *NDMT* rigid plate is instrumented so that pressure and displacement can be measured directly.

This paper is based on the *NDMT* testing in the typical alluvial deposits of the Punjab province of Pakistan which consist of silty sand/fine sand. In order to correlate the *NDMT* test results with those of other conventional methods, Standard Penetration Tests (SPTs) were carried out at locations close to the *NDMT* testing locations. The disturbed soil samples recovered in the split spoon sampler were used to determine the grain size distribution and direct shear strength parameters.

The *NDMT* indices viz. material index ( $I_D$ ), dilatometer modulus ( $E_D$ ), and horizontal stress index ( $K_D$ ) have been evaluated from the corrected load – deformation curves of each *NDMT* test. Subsequently, new correlations for the dilatometer indices have been developed with conventional soil characteristics such as drained shear strength ( $\phi'$ ) and elastic modulus ( $E$ ) for the Punjab sandy subsoils.

## 1 INTRODUCTION

The evaluation of strength and deformation characteristics of soil deposits has always been an area of key interest for design engineers. A host of techniques have been developed, over the years, for representative sampling, laboratory testing and in-situ testing. While it is possible to sample all soils the quality of the samples depends on the type of soil and the sampling technique. This means that it is often difficult to obtain representative samples for laboratory testing. This is one reason that in situ tests are used.

Ever since the appearance of the first in situ test, the penetration test, engineers and scientists have continuously endeavored to improve the equipment, the test protocol and the interpretation to obtain more representative values of in-situ strength, stiffness and stress. This has led to an improvement in the analyses required for the design of foundations and cut slopes.

Like other engineering techniques used in the evaluation of geotechnical design parameters, intrusive in-situ testing does disturb the ground to

some extent creating difficulties in interpreting tests to obtain intrinsic design parameters. This difficulty in the interpretation of test results is primarily due to the complex behaviour of soils, together with the lack of control and choice of the boundary conditions in any field test. Therefore the results of many in situ tests are interpreted using empirical correlations with results of laboratory tests.

One such test is the Marchetti dilatometer test. The original Marchetti dilatometer (*MDMT*) is a simple device that can be used to determine in-situ stress, stiffness and strength of a soil with some degree of confidence. However, the *MDMT* is not robust enough to test stony soils such as residual soils and glacial till, as the membrane can tear. It is for this reason that a new blade has been developed that can be used in a greater variety of soils. The new dilatometer, the *NDMT* has been found to be more robust than the *MDMT* as it has been used in a variety of difficult soils. Akbar (2001) presents the design of the *NDMT* together with in-situ testing procedures, data analysis techniques and comparison of the results with those from the *MDMT*.

This paper describes the results of testing the non-cohesive soils with the *NDMT* at a site near Jaranawala city of Pakistan to improve correlations

between the *NDMT* indices and soil properties and geotechnical design parameters.

## 2 THE NEWCASTLE FLAT DILATOMETER (*NDMT*)

The *NDMT* blade is shown as (i) in Fig. 1 where the piston that loads the soil during a test is shown as (ii). Fig. 2 shows the components in the piston assembly. The use of the wave spring washer (iii in Fig. 2) between the piston flange (ii) and the retaining ring (iv) keeps the piston flush with the blade until the piston is pressurized using dry  $N_2$  gas and returns the piston to its at rest position when depressurized. Two O-rings are incorporated in the *NDMT* to keep the assembly air and water-tight. The applied gas pressure is recorded using a pressure transducer.

A Hall Effect Transducer (*HET*) is used to measure the displacement of the piston. The magnet is fixed at the center of moving piston while the *HET* is fixed to the body of the blade in front of the magnet. When the piston moves by internally pressurizing the blade, the *HET* produces a change in its output according to the flux intensity. This output is non-linear but non-hysteretic and a second-degree curve fits the data as shown in Fig. 3. Access to the connections between the *HET* and the cable is via steel cover plate (iii in Fig. 1). The output of the pressure transducer and the *HET* are read and recorded by a computer. The blade is either jacked or pushed to the test level.

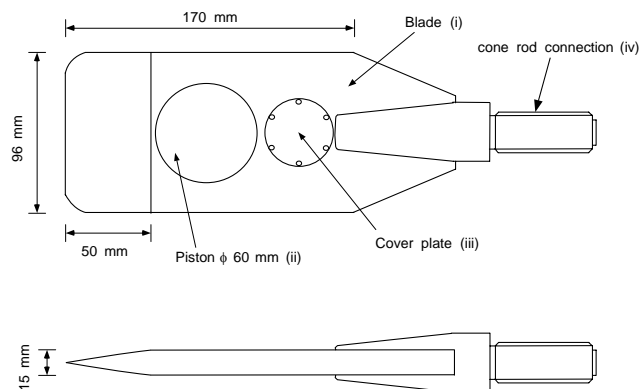


Figure 1 The Newcastle flat rigid dilatometer (*NDMT*)

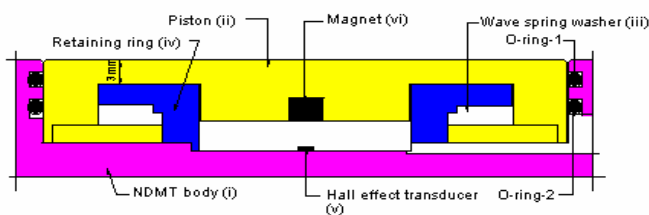


Figure 2 Piston assembly of the *NDMT*.

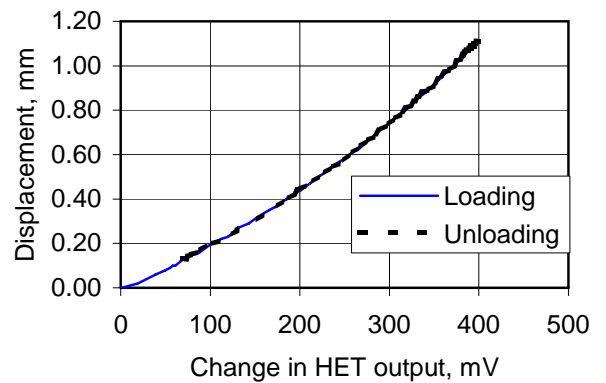


Figure 3 A typical data plot for the *HET* in the *NDMT*.

## 3 SITE OPERATIONS

The Newcastle dilatometer testing was carried out at a site near Jaranwala, district Faisalabad, Pakistan. The *NDMT* equipment was assembled on-site as shown in Figure 4. The system compliance calibration needed to correct for the pressure required to overcome the stiffness of the wave spring was carried out by increasing the gas pressure at a constant rate i.e. similar to that for the Marchetti *DMT*. Figure 5 shows a typical plot for system compliance calibration. The maximum pressure required to move the piston by 1.1 mm is less than 90 kPa. This is comparable with that required to inflate the *MDMT* membrane.

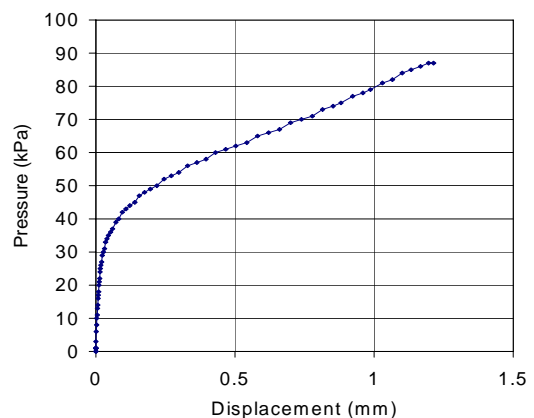


Figure 5 A typical calibration data plot for the *NDMT* system compliance

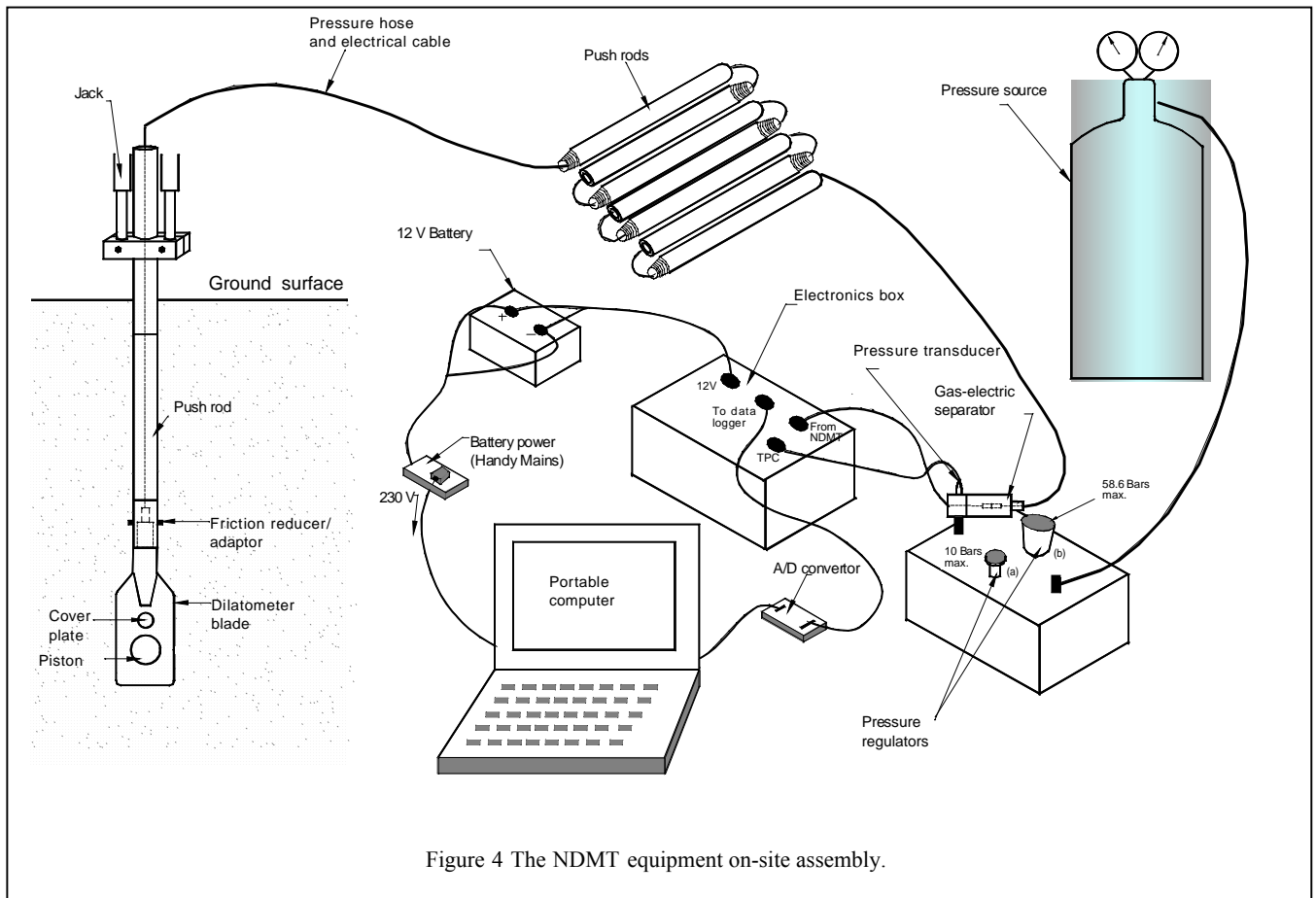


Figure 4 The NDMT equipment on-site assembly.

After the calibration, the probe was pushed into the ground using a hydraulic jack. The reaction force was obtained through a heavy-duty frame loaded with sand bags. During the testing, the pressure was applied through a needle valve pressure regulator. After attaining 1.1 mm movement of the piston, the pressure was vented off. Each test took between 1 and 3 minutes. No unload-reload cycles during tests were included in this study. At the end of testing at each location, the instrument was withdrawn and calibrated for system compliance. The calibrations before and after the in-situ testing were averaged. The in-situ pressure deformation curves were then corrected for system compliance.

The *NDMT* tests were carried out at every 20 cm interval as recommended by Marchetti (1980) at three locations to depths varying between 6 m and 9 m below the existing surface level. In all, 84 tests were performed in the three holes.

In order to correlate the *NDMT* data with other techniques, *SPT* testing was also carried out adjacent to the *NDMT* test locations on the same site. Fig. 6 shows plots of *SPT* blows (*N*-values) against depth for the three test locations. Subsoil samples were recovered from the *SPT* for determining various properties in the laboratory.

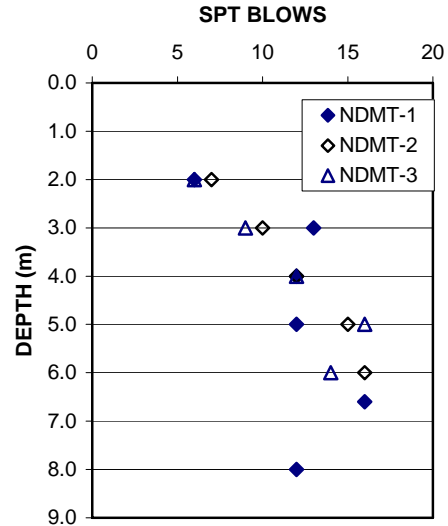


Fig. 6 Plot of SPT blows against depth.

#### 4 INTERPRETATION OF TEST DATA

The field test records and the laboratory testing results have revealed that the subsoils comprise fine sand with varying amounts of silt content and are in loose to medium dense state within the depth explored. The ground water table was encountered at 3.50 m depth below the existing ground level.

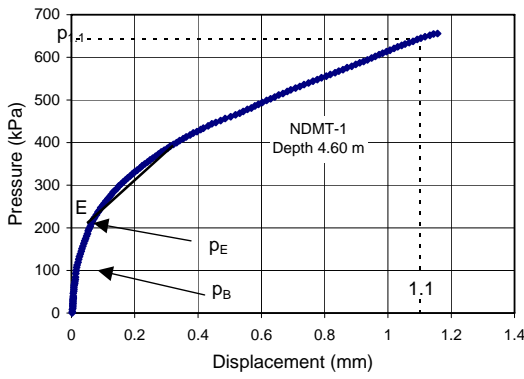


Figure 7 A typical NDMT test curve

the blade into the soil causes the soil to yield, which implies the initial pressure on the piston should be  $p_E$ . The fact that the initial pressure ( $p_B$ ) is less than  $p_E$  is a result of unloading that occurs; as the soil is unloaded as it moves past the shoulder of the blade.

The piston is forced to move by at least 1.1 mm and the pressure corresponding to this displacement is recorded as  $p_{1.1}$ , which is an equivalent to Marchetti DMT  $p_1$  pressure.

The three pressures ( $p_B$ ,  $p_E$  and  $p_{1.1}$ ) together with the effective overburden pressure and in-situ static pore water pressure at the test depth were

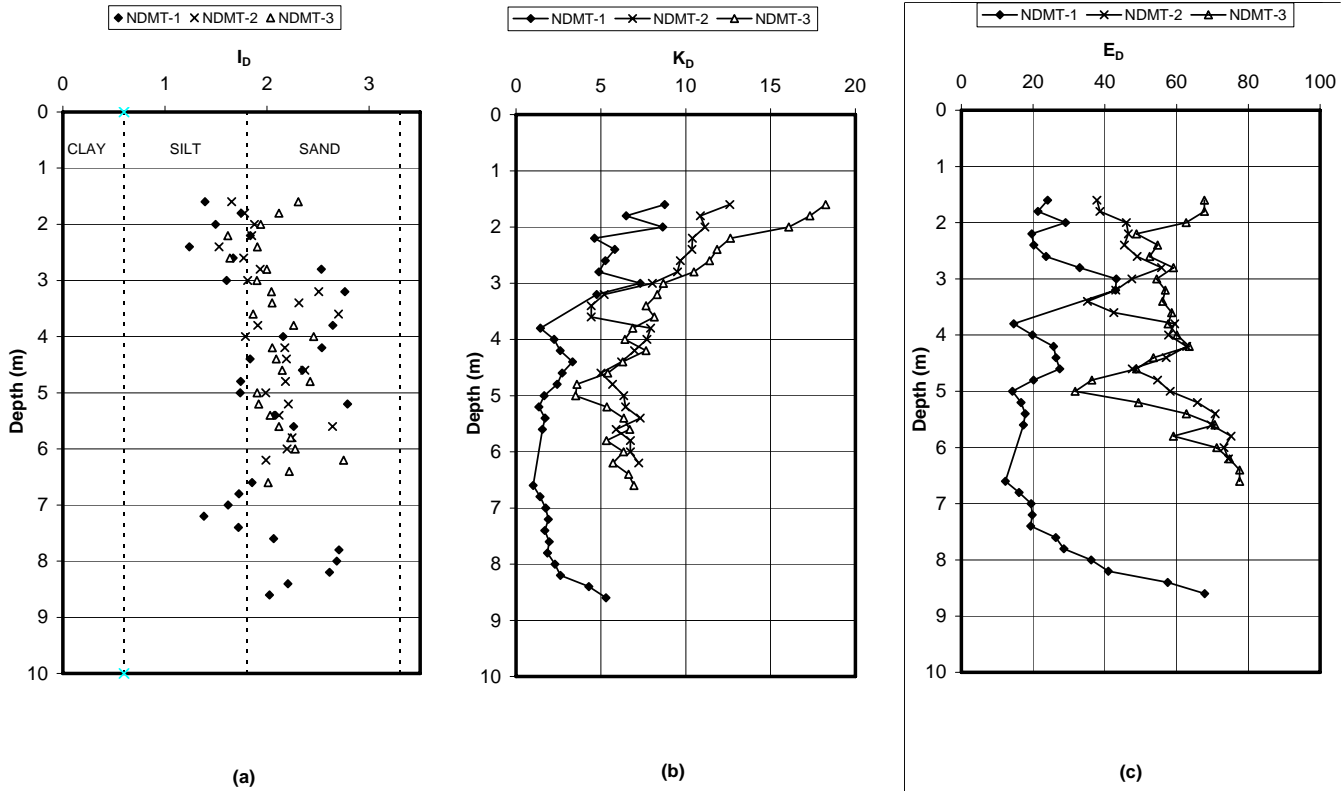


Fig. 8 Plot of dilatometer indices vs. depth for the three NDMT locations

The data points for each NDMT test were plotted after being corrected for system compliance. Fig. 7 shows a typical corrected test curve. The corrected load-deformation curves of each NDMT test have been analyzed to find the representative pressures ( $p_B$ ,  $p_E$  and  $p_{1.1}$ ) and the appropriate indices ( $I_D$ ,  $K_D$  and  $E_D$ ), as discussed in the following sections.

$p_B$ , (Fig. 7) represents that pressure on the load-displacement curve where the piston just starts to move. This can also be termed the take-off pressure. The yield pressure  $p_E$  (equivalent to Marchetti DMT  $p_o$  pressure) has been determined by tracing back the trend of (or tangent to) the initial part of the loading curve to intercept the pressure axis at point E. This pressure corresponds to zero displacement of the piston, that is when the piston is flush with the blade. Note that pushing

converted to horizontal stress index ( $K_D$ ), material index ( $I_D$ ) and dilatometer modulus ( $E_D$ ), using the following equations:

$$K_D = \frac{p_E - u_o}{\sigma'_v} \tag{1}$$

$$I_D = \frac{p_{1.1} - p_E}{p_E - u_o} \tag{2}$$

$$E_D = 42.8(p_{1.1} - p_B) \tag{3}$$

These indices are plotted against depth in Fig. 8. The interpretation of these indices for the soils of this site is briefly discussed as below:

#### 4.1 Material Index, $I_D$

The particle size distribution analyses performed in the laboratory indicate that the soils are predominantly fine sands with fines varying between 3 and

40 % within the *NDMT* test depths (Fig. 9). The  $I_D$  values determined using eq. 2 show close agreement to soil classification established from the sieve analyses. The  $I_D$  values for all the three *NDMT* soundings are plotted against depth and shown in Fig. 8(a). These values range between 1.3 and 2.8 indicating the subsoils to vary from sandy silt to silty sand using the classification chart of Marchetti and Crapps (1981).

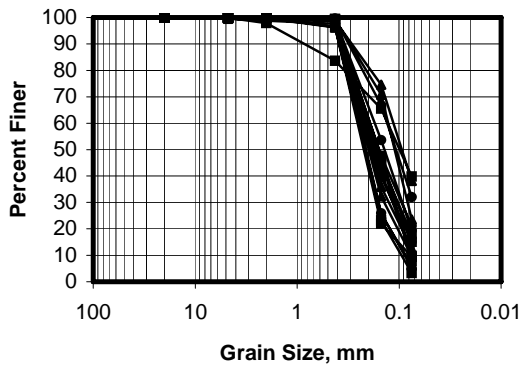


Fig. 9 Particle size distribution curves for the subsoils at the site.

#### 4.2 Horizontal Stress Index

$K_D$  gradually decreases with depth, becoming nearly constant below a depth of 3.5m as shown in Fig. 8(b). This trend may be due to the desiccation effects near the ground surface. The  $K_D$  values at the three locations vary between 8.8 and 1.0, 12.6 and 4.4, 18.3 and 3.5 respectively.

#### 4.3 Dilatometer Modulus

The dilatometer modulus values have been determined using eq. (3) and are plotted in Fig. 8(c). The  $E_D$  values for the three locations range from 12 to 68, 35 to 75 and 32 to 78 (MPa). In general, the  $E_D$  values are increasing with depth indicating an increase in stiffness of soil though there are a few inter bedded weak layers giving lower values.

The correlations developed using the data obtained from the field and laboratory tests are discussed in the following sections:

#### 4.4 Soil Identification and Unit Weight

The data obtained from this research are plotted on the Marchetti and Crapps (1981) chart, Fig. 10(a, b) and the following conclusions have been drawn.

- The  $I_D$  values plot in silty sand zone with a few values in sandy silt zone. This agrees with the sieve analysis results (Fig. 10a).
- The  $E_D$  values for borehole *NDMT*-1 are lower than those for the other boreholes. This is due to weak subsoil conditions at this location. The fact that it was easier to jack the *NDMT* blade

into the ground at *NDMT*-1 location compared to the other two locations supports this finding.

- Plot of  $E_D$  and  $I_D$  values on the Marchetti and Crapps (1981) chart shows unit weight values higher than those obtained from correlations based on SPT blow count (Bowles, 1988). Settlement predictions based on the assumption that a foundation is flexible are adjusted by a factor of 0.8 to allow for the actual rigid behaviour. Thus a coefficient of 0.8 has been used to produce Figure 10b which gives a better fit the Marchetti and Crapps (1981) soil classification chart.

#### 4.5 Drained Friction Angle, $\phi'$

The angle of friction is related to the soil type and density of the soil which, in the case of dilatometer tests is a function of  $I_D$  and  $K_D$ . Fig 11 shows the dilatometer data plotted against the angle of friction obtained from laboratory tests. There appears to be two trend lines which suggests that there may be a correlation between the dilatometer data and angle of friction. This is reinforced when the empirical  $\phi'$  values derived from the SPT tests are included. Further, these lines are parallel with a slope of 0.173. This suggests that there may be a relationship between the indices and the angle of friction of the form:

$$\phi' = 0.173 (I_D \times K_D) + \text{constant}$$

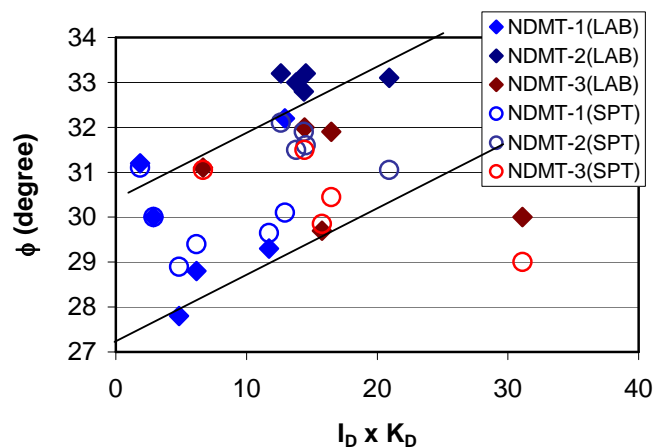
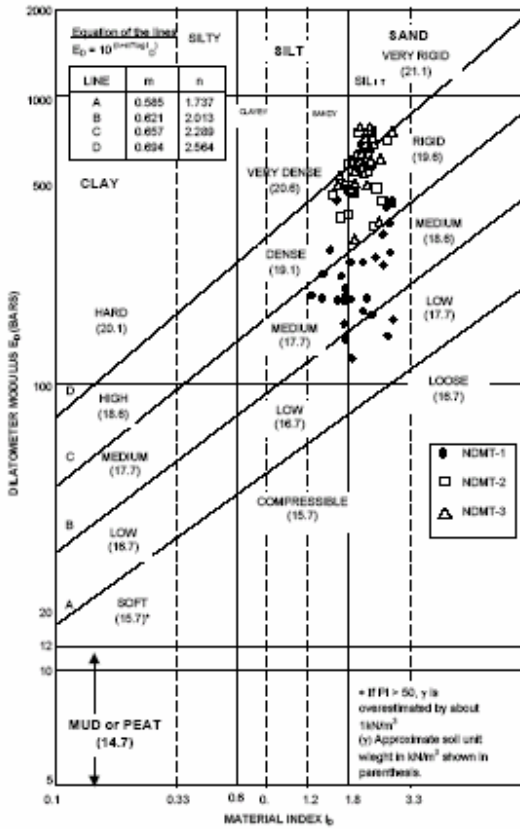
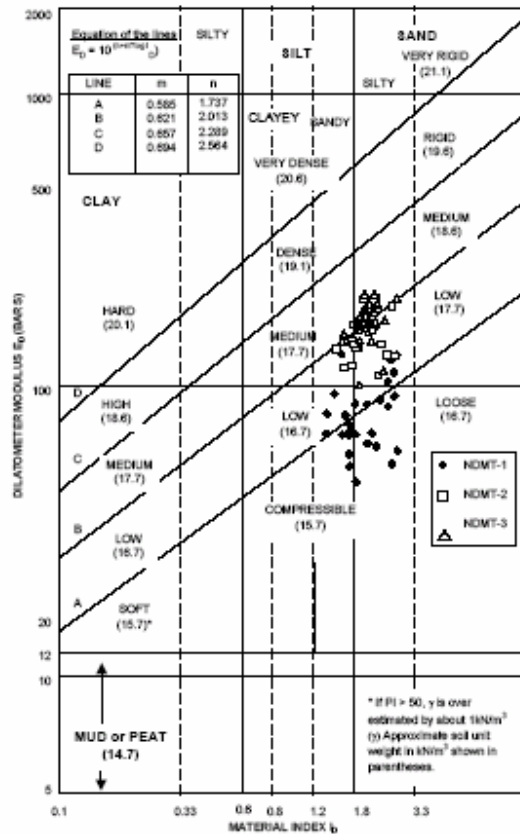


Fig. 11 dilatometer data plotted against the angle of friction obtained from laboratory tests

Note that this relationship does not take into account the density of the soil. However, the constant may be a function of density given that the data clustered about the lower line are either tests at shallow depths or in soil that has a low stiffness (see Fig. 8). Further data are needed to validate this model.



(a) Plot of the NDMT data on Marchetti and Crapps (1981) chart



(b) Plot of the NDMT data using multiplier coefficients of 0.85 for  $E_D$  on Marchetti and Crapps (1981) chart

Fig. 10 Plot of NDMT data on the Marchetti and Crapps (1981) chart

#### 4.6 Elastic Modulus

The modulus of elasticity  $E$  and the Dilatometer Modulus  $E_D$  are related by the following formula (Marchetti, 1980).

$$E = (1 - \nu^2)E_D \tag{4}$$

For silty sands taking  $\nu = 0.4$  (Bowles, 1988)

$$\text{then } E = 0.84E_D \tag{5}$$

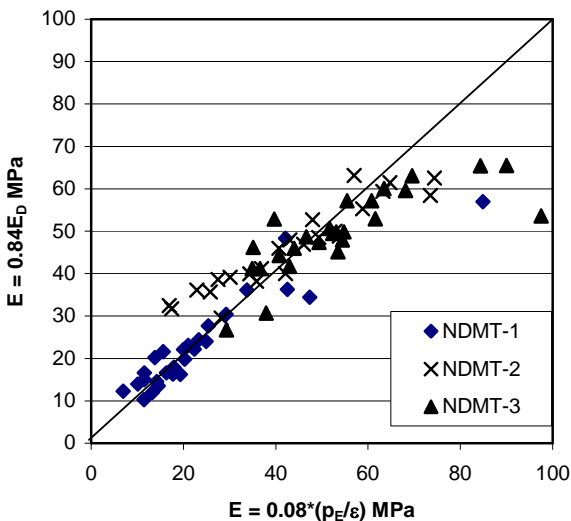


Figure 12 Comparison of Elastic Moduli values

The initial part of the loading curve corresponds to reloading of the soil that has been unloaded during installation. Therefore it is an elastic response. The values of  $E$  calculated using eq. (5) are plotted in Fig. 12 against the ratio between the yield pressure,  $p_E$ , and the strain defined as the displacement corresponding to  $p_E$  divided by half the thickness of the  $NDMT$  blade. A good agreement between the two approaches suggests using the following relation to determine modulus of elasticity from the initial part of the  $NDMT$  curve.

$$E = 0.08(p_E/\epsilon) \tag{6}$$

where,  $\epsilon = (\text{displacement}) \div 7.5$

This relationship needs to be validated against results of other types of tests and observations of soil behaviour and be extended to cover other soil types.

#### 5 OTHER SALIENT FEATURES OF NDMT

There are a number of features of the  $NDMT$  that enable repeatable and consistent results to be obtained:

- The  $HET$  output is stable and unaffected by any change in temperature.

- The *NDMT* piston assembly is relatively straightforward.
- The movement if the piston is monitored during a test which produces a pressure displacement curve that may be analyzed using cavity expansion theory.
- Unload reload cycles can be included to provide further information on the elastic response of the ground.

## 6 CONCLUSIONS

The following conclusions are drawn from the analysis of *NDMT* tests in silty sand in conjunction with results from the SPT and laboratory tests.

1. The soil classification chart of Marchetti and Crapps (1981) can be used to classify and estimate the unit weight of the soil after applying a correction of 0.80 to  $E_D$ .
2. There is a relationship between the angle of friction obtained from laboratory tests and the material and horizontal stress indices. This is supported by the angles of friction derived from SPT data which suggests that the indices are appropriate.
3. The initial loading portion of the *NDMT* test is the elastic response of the ground. The value of stiffness derived from this portion compares favorably with that derived using the Marchetti formula.

Further tests on different soil types are needed to establish whether these correlations are site specific or generic.

## REFERENCES

- Akbar, A. (2001): Development of Low Cost In-situ Testing Devices, *Ph.D. Thesis*, Civil Engineering Department, University of Newcastle, UK.
- Akbar, A. and Clarke, B.G. (2001): A Flat Dilatometer to Operate in Glacial Tills, *Geotech. Testing Journal*, GTJODJ, Vol. 24, No.1, pp. 51-60.
- Akbar, A. and Clarke, B.G. (2002): A New Robust Device for the Identification of Potential Slip Surfaces, 3<sup>rd</sup> Int. Conf. On Land Slides, Slope Stability and the Safety of Infra Structures, July 11-12, 2002, Singapore.
- Bowles, J.E. (1988). *Foundation analysis and Design*, 4<sup>th</sup> ed. McGraw Hill International edition
- Campanella, R.G. and Robertson, P.K. (1991): Use and Interpretation of a Research Dilatometer, *Canad. Geotechn. Journal*, Vol. 28: 113-126.
- Marchetti, S. (1980): In Situ Tests by Flat Dilatometer, *J. Geotech. Engng. Div., ASCE*, Vol. 106, No. GT 3, pp.299-321.
- Marchetti, S. and Crapps, D.K. (1981), "Flat Dilatometer Manual," *GPE Inc., USA*.
- Marchetti, S. (1997): The Flat Dilatometer Design Applications, *Proceedings, Third Geotechnical Engng. Conference, Cairo University, Egypt*, pp. 1-25.